Numerical Simulation of Realistic Blocking and Local Lyapunov Stability Analysis of the Barotropic Prediction Model

H. L. Tanaka and Daisuke Nohara
Institute of Geoscience
University of Tsukuba
Tsukuba, 305 Japan

1. Introduction

The extended-range numerical weather prediction has been hampered by the predictability barrier caused by the chaotic nature of large-scale turbulent flow. The initial error tends to grow rapidly due to the instability included within the model. Recently, we have constructed a new type of prediction model which excludes the major dynamical instability. It is demonstrated that this model can simulate realistic atmospheric blocking which often persists more than two weeks. We have shown in our previous report (Tanaka and Nohara, 1997) that the model has a predictability somewhere around 35 days. Hence, the pronounced blocking in the model is well predictable two weeks in advance within the model atmosphere.

The purpose of this study is to demonstrate the slow error growth in the model atmosphere at the energetically saturated stage. The slow error growth is compared with rather fast growth when baroclinic instability dominates in the model atmosphere. Lyapunov stability analysis is then performed for these two cases to find quantitatively the growth rate of the prediction error.

2. Model description

The model description is detailed in Tanaka et al. (1996). A system of primitive equations with a spherical coordinate may be represented in terms of the 3-D spectral expansion coefficients:

$$\frac{dw_i}{d\tau} + i\sigma_i w_i = -i \sum_{jk} r_{ijk} w_j w_k + s_i, \quad i = 1, 2, 3, \ldots \quad (1)$$

where τ is a dimensionless time, the symbol σ_i denotes the eigenfrequency of the normal mode at a resting atmosphere, and r_{ijk} is the interaction coefficient for nonlinear wave-wave interactions. In this study, we attempt to construct a spectral barotropic model, using only the barotropic components of w_i retaining only the low-frequency Rossby mode basis. The spectral truncation of the model corresponds to R20. In this study, we consider the following physical processes:

$$s_i = (BC)_i + (TF)_i + (DF)_i + (DZ)_i + (DE)_i, \quad (2)$$

where $(BC)_i$ represents the baroclinic instability, $(TF)_i$ the topographic forcing, $(DF)_i$ the biharmonic diffusion, $(DZ)_i$ the zonal surface stress, and $(DE)_i$ the Ekman pumping for eddies.

3. Result

The model is first integrated for 1000 days with the standard parameter set. Large-scale blockings appears one after another in the model atmosphere. Figure 1 illustrates geopotential height at day 338, where a pronounced dipole blocking occurs over Europe. The configuration with high-low vortex pair and the persistency lasting more than 10 days are satisfactory as a simulation of a blocking.

Next, an experiment run is performed by removing topography to isolate the exponential growth due to the linear baroclinic instability parameterized in the model. Eddy energy level increases exponentially from the infinitesimal noise for the first 50 days, then the energy level saturates near the mean level. The energy balance is maintained by the source due to baroclinic instability at the synoptic waves and nonlinear scattering toward the rest of the waves. The energy increases most rapidly at around day 30 for this experiment. For this reason, we superimpose a small error (approximately 2% in energy level) on the day 30 to see if the error grows rapidly as fast as the baroclinic instability. Figure 2 illustrates the error growth for the prediction run (solid line) and that for a persistency forecast (dashed line). The prediction error is measured by the global error energy defined by the difference of the spectral coefficients of the experiment run $\bar{w}_i$ and the prediction run w_i:

$$E_i = \frac{1}{2} p_s h_0 |w_i - \bar{w}_i|^2 \quad (3)$$

where, p_s and h_0 denote surface pressure and equivalent depth of the reference state. The total error energy is evaluated as the sum of E_i over all waves. It is found that the error grows as fast as the baroclinic instability exceeding the persistency forecast after 5 days.

Next, the same experiment run is repeated with topography. The initial axisymmetric flow is soon saturated by disturbances after about 20 days of time integration for this mountain run. We then superimpose a small error on the day 30 to see if the error grows rapidly as in the previous example. The resulting error growth is presented in Figure 3. The error does not grow in this experiment as in our previous report (Tanaka and Nohara, 1997), supporting the conclusion that the predictability is near 35 days.

4. Lyapunov stability analysis

Local Lyapunov stability analysis is performed in this study to find the exponential growth rate of the initial error at the day 30. For the prediction interval of 5 days, we found that the values of local Lyapunov exponents are 1.22 day^{-1} for the no-mountain run and 0.34 day^{-1} for the mountain run. Although the value of the no-mountain run is reasonably large, that of the mountain run is also too large to describe the predictability of 35 days. The corresponding Lorenz indices appear to be 32.1 and 0.96, respectively. The result suggests that the error volume around the initial solution trajectory has decreased for the prediction interval of 5 days in the mountain run.

5. Discussion

The present study shows an interesting result in the predictability limit associated with chaos. The result of this study demonstrates that the error growth is controlled by the dynamical instability within the model. The prediction error grows as fast as baroclinic instability when the atmospheric energy increases exponentially by the dominant linear process. However, the prediction error does not grow much after the saturation in the energy level. A detailed study of this model suggests that the moderate speed of error growth is soon saturated by the higher-order nonlinear effect. It is quite interesting to note that the nonlinear term acts to reduce the exponential growth of error in the tangent linear system.

References

Tanaka, H.L., K. Kimura, and T. Yasunari, 1996: Time spectral analysis for the natural variability of the barotropic model atmosphere with annual cycle. *J. Meteor. Soc. Japan.*, 74, 909 – 921.

Tanaka, H.L. and D. Nohara, 1997: Medium-range numerical weather prediction by a simple barotropic model with parameterized baroclinic instability. WMO Weather Prediction Research Programmes, No.25, 6.31–6.32.

This research was partly supported by the Environmental Research Fund from Asahi Beer.

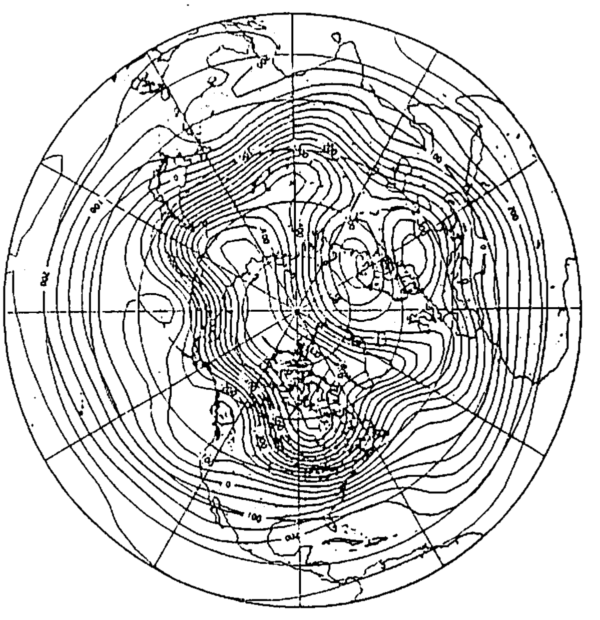

Fig. 1 Geopotential height for day 338, indicating typical dipole blocking over Europe.

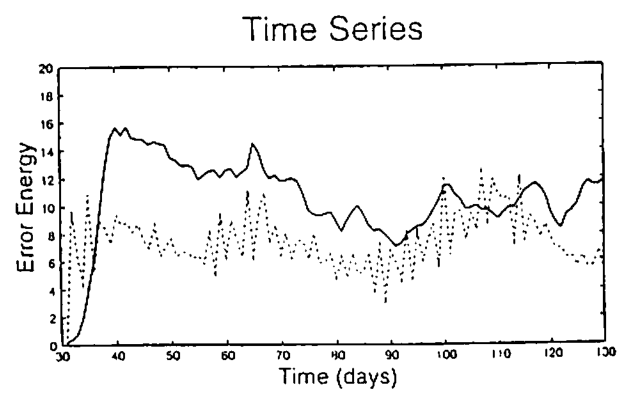

Fig. 2 Time series of error energy for the prediction run (solid line) and persistency forecast (dashed line) starting from day 30 for the no-mountain run.

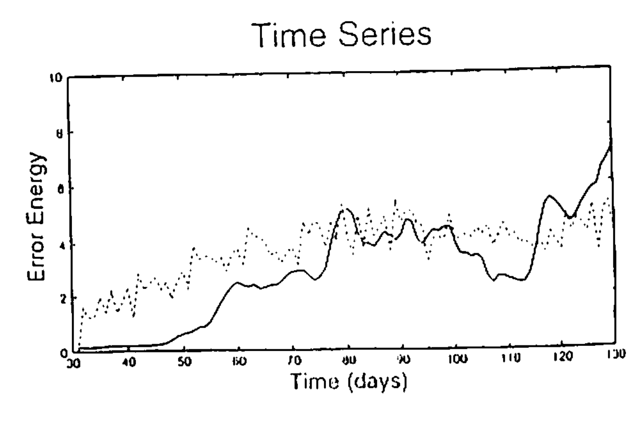

Fig. 3 As in Fig. 2 but for the mountain run.